What are Marine Ecological Time Series telling us about the ocean? A status report

[Individual Chapter (PDF) download]

The full report (all chapters and Annex) is available online at:

http://igmets.net/report

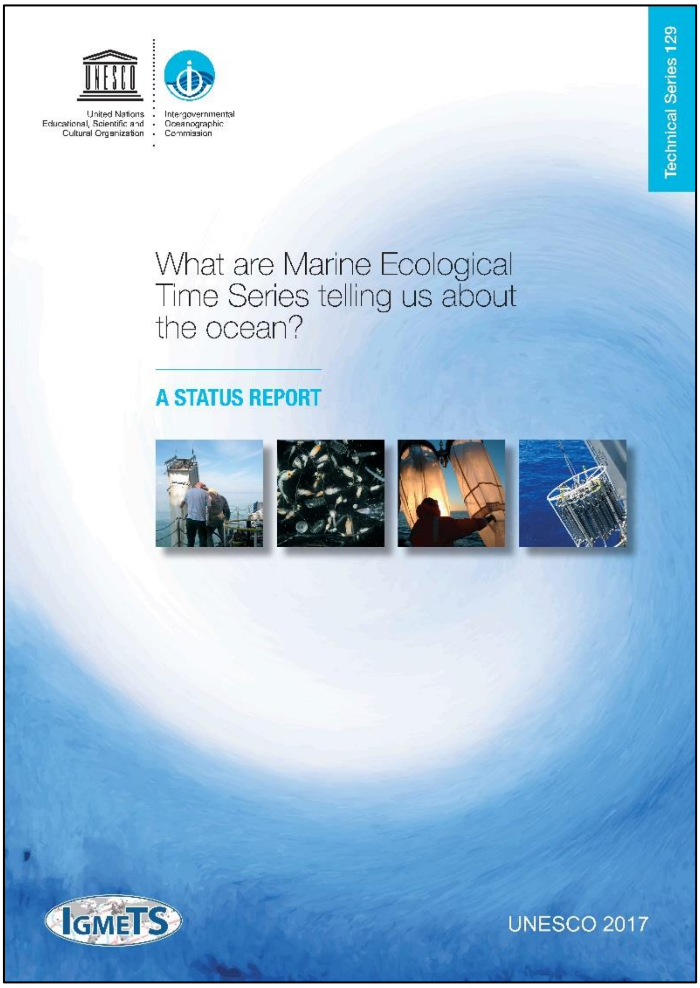

This page intentionally left blank

to preserve pagination in double-sided (booklet) printing

8 South Pacific Ocean

Peter A. Thompson, Todd D. O'Brien, L. Lorenzoni, and Anthony J. Richardson

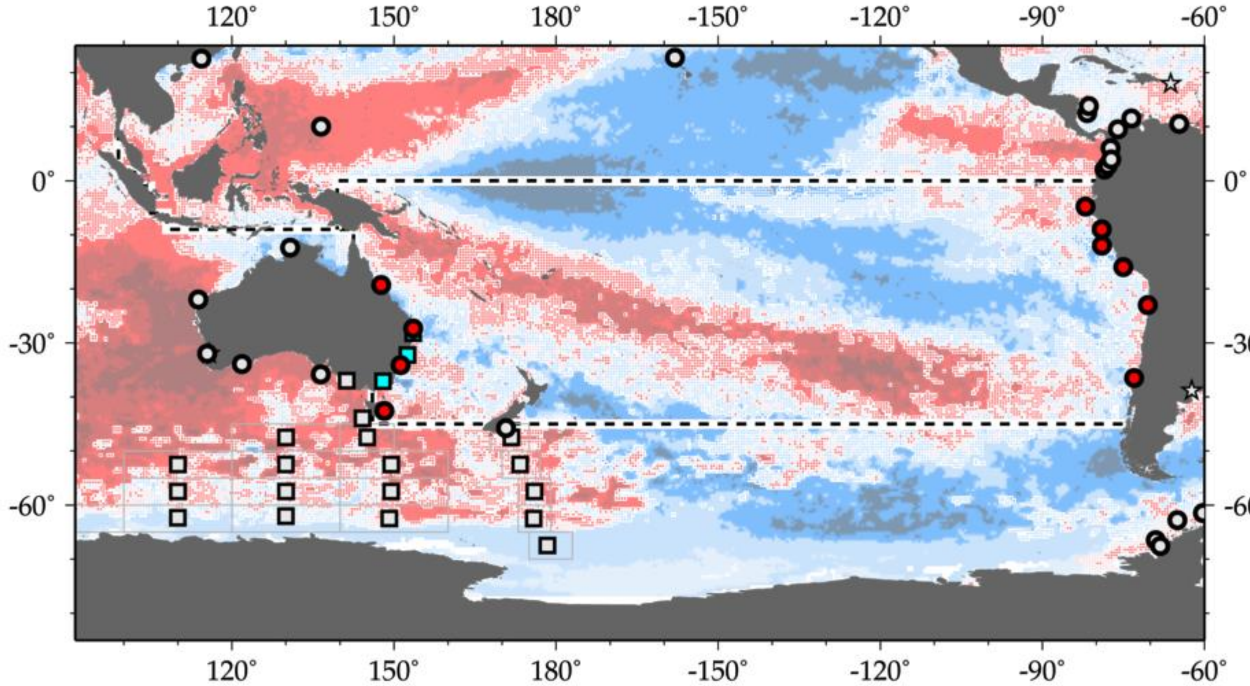

Figure 8.1. Map of IGMETS-participating South Pacific time series on a background of a 10-year time-window (2003–2012) sea surface temperature trends (see also Figure 8.3). At the time of this report, the South Pacific collection consisted of 13 time series (coloured symbols of any type), of which three were from Continuous Plankton Recorder surveys (blue boxes) and none were from estuarine areas (yellow stars). Dashed lines indicate boundaries between IGMETS regions. Uncoloured (gray) symbols indicate time series being addressed in a different regional chapter (e.g. Southern Ocean, North Pacific, Indian Ocean). See Table 8.4 for a listing of this region's participating sites. Additional information on the sites in this study is presented in Annex A.6.

Participating time-series investigators

Patricia Ayon, Frank Coman, Claire Davies, Ruth Eriksen, Ruben Escribano, Jesus Ledesma Rivera, Felicity McEnnulty, Anthony J. Richardson, Anita Slotwinkski, Mark Tonks, and Julian Uribe-Palomino

This chapter should be cited as: Thompson, P. A., O'Brien, T. D., Lorenzoni, L., and Richardson, A. J. 2017. The South Pacific Ocean. I*n* What are Marine Ecological Time Series telling us about the ocean? A status report, pp. 133–151. Ed. by T. D. O'Brien, L. Lorenzoni, K. Isensee, and L. Valdés. IOC-UNESCO, IOC Technical Series, No. 129. 297 pp.

8.1 Introduction

After the North Pacific, the South Pacific Ocean (Figure 8.1) is the second largest body of water considered in this report. The surface currents of the South Pacific are strongly influenced by the predominantly westerly wind near the southern boundary (45°S) and easterly winds near the equator (Figure 8.2). Along the southern boundary of the South Pacific, strong easterly flow is found at the subtropical front (STF) and in the Antarctic Circumpolar Current (ACC). The westward return flow is primarily by the South Equatorial Current (SEC) (Figure 8.2; Roemmich and Cornuelle, 1990). A portion of the easterly flow passes between South America and Antarctica, but part of it curves northward and flows along the west coast of South America as the Humboldt (or Chile–Peru) Current. The quasi stationary South Pacific high atmospheric pressure zone near 100°W, between 20 and 35°S, deflects winds toward the equator and contributes to the ~15 Sv (Sv = sverdrup = 10^6 m^3 s^{-1}; Wijffels *et al*., 2001) strength of the Humboldt Current (Wyrtki, 1963), one of the most productive eastern boundary currents (EBCs) in the global oceans. Strong wind-induced upwelling along the Peru and Chile coastlines results in large phytoplankton blooms, a substantial biomass of zooplankton, and some of the world's largest annual fish catches (Fiedler *et al*., 1991; Daneri *et al*., 2000; Pennington *et al*., 2006; Chavez and Messié, 2009; Correa-Ramirez *et al*., 2012).

The Humboldt Current bifurcates around 25°S (Fuenzalida *et al*., 2008); the offshore branch heads northwest and the more coastal branch continues along the coast of Peru. Both branches eventually turn mainly westward as part of the SEC that flows from South America to the western Pacific. The SEC divides as it approaches Australia producing at least three major branches, one of the most important being the East Australian Current (EAC). The EAC is the Western Boundary Current (WBC) of the southwestern Pacific and is associated with the South Pacific subtropical gyre (Mata *et al*., 2000). The EAC is significantly weaker than other WBCs in terms of volume transport, with ca. 15 Sv mean annual flow (Mata *et al*., 2000). It flows poleward along the eastern Australian coast carrying warm water from tropical to mid latitudes. It separates from the continent at 30–34°S, where about two-thirds of the flow moves eastward and then continues down the east coast of New Zealand before going farther eastward (Godfrey *et al*., 1980; Ridgway and Godfrey, 1997). In the region where the EAC

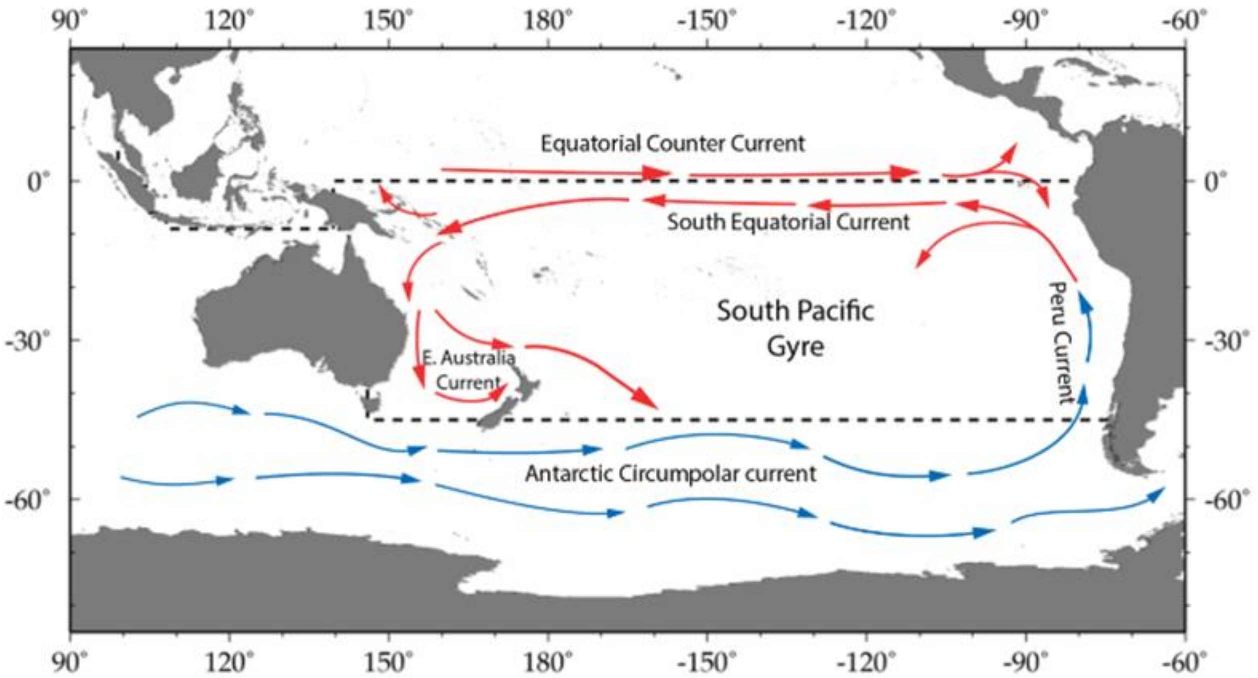

Figure 8.2. Schematic major current systems in the IGMETS-defined South Atlantic region. Red arrows indicate generally warmer water currents; blue arrows indicate generally cooler water currents.

veers eastward, the remaining ca. one-third of the EAC continues south past Tasmania as an eddy field (Mata *et al*., 2006; O'Kane *et al*., 2011; Macdonald *et al*., 2013; Cetina-Heredia *et al*., 2014). The seasonal, interannual and decadal changes of the EAC, together with the high variability induced by the mesoscale eddies, dominate circulation features along the east coast of Australia and influence the biogeochemistry and ecology of the region (Cetina-Heredia *et al*., 2014).

In the western tropical Pacific between 10°Nand 10°S and centred around 170°E, the Pacific Warm Pool (WP) is characterized by high sea surface temperatures (SST, 28–29°C) and low sea surface salinities (SSS, <35), the latter induced by heavy rainfall (Wyrtki, 1989). Along much of the northern edge of the South Pacific and extending into the central gyre is a large region of very high solar radiation (ca. 200 W m^{-2}), warming the ocean, causing considerable evaporation, and producing large net precipitation along the intertropical convergence zone (ITCZ) near the equator (Meehl *et al*., 2008). Farther south at ca. 15–25°S and centred at ca. 124°W, the warming produces a region of very high net evaporation and high surface salinities (SSS >36; Hasson *et al*., 2013). This pool of high-salinity water seasonally migrates eastward during austral summer and westward during austral winter, driven by changes in the intensity of the South Pacific Convergence Zone and easterly winds. However, a net migration westward of the salinity maximum over the past 20 years has been noted (Hasson *et al*., 2013).

A high pressure zone tends to persist over Australia during austral summer (December–February), directing winds that deflect equatorial trade winds poleward and creating the strong South Pacific Convergence Zone (SPCZ) (Vincent, 1994; Vincent *et al*., 2011). While the SPCZ is best developed during austral summer, it is present year-round, extending from New Guinea (0° 150°E) east–southeastward to about 30°S 120°W. In its northwestern sector, the SPCZ merges with the Intertropical Convergence Zone (ITCZ). This low-level atmospheric convergence and precipitation zone is one of the major components of South Pacific climate and is responsible for a large fraction of South Pacific precipitation, especially during austral summer (Vincent, 1994; Brown *et al*., 2011; Vincent *et al*., 2011).

Important drivers of oceanic ecology such as currents, upwelling, tides, irradiance, temperature, and nutrients show significant variation across a range of time- and space scales producing a complex spatial and temporal pattern of trends. This report focuses on time-scales of 5–30 years and spatial scales from hundreds to millions of square kilometers. Most of the multiyear and large spatial-scale variability in the physics, biogeochemistry, and ecology of the South Pacific is modulated by "shorter" natural climatic cycles such as El Niño Southern Oscillation (ENSO), the Interdecadal Pacific Oscillation (IPO), and Southern Annular Mode (SAM). These natural cycles often have a more profound effect on SST differences between years than the long-term rise of ca. 0.03°C $decade^{-1}$ since 1850 (Rayner *et al*., 2006).

El Niño Southern Oscillation (ENSO) is a coupled ocean and atmosphere cycle consisting of a weakening and strengthening of the easterly trade winds over the tropical Pacific and with a consequent impact on sea surface temperatures (Wang *et al*., 2012a). It fluctuates between warm (El Niño) and cold (La Niña) conditions in the tropical Pacific (Rayner *et al*., 2003; McPhaden *et al*., 2006; Annex A6). During El Niño, the easterly trade winds weaken, the reduced westward flow at the equator results in the migration of warm surface water eastward, and the upwelling along the west coast of South America substantially decreases. La Niña is characterized by stronger trade winds, warmer surface waters in the western Pacific, and cold water at the equator in the central and eastern Pacific (Rasmusson and Carpenter, 1982; Philander, 1990; Trenberth, 1997; Pennington *et al*., 2006). ENSO affects many other regions through teleconnections in the atmosphere and ocean and tends to cycle between 2–7 years (McPhaden *et al*., 2006). Depending on the temporal window and region selected, this cycle can make the surface ocean warmer or colder.

The Interdecadal Pacific Oscillation (IPO) is a pattern of Pacific climate variability similar to ENSO in character, but which persists for much longer. It is a robust, recurring pattern centred over the mid-latitude Pacific basin with a 20–30-year period (Biondi *et al*., 2001). During negative IPOs, the SPCZ moves southwest, similar to La Niña events (Folland *et al*., 2002). The recent hiatus in global warming has been associated with a persistent negative IPO that commenced in about 2000 (Dai *et al*., 2015; Trenberth, 2015). In late 2014, there were signs that the IPO might be shifting to a more positive phase.

During a positive Southern Annular Mode (SAM) event, the southern hemisphere westerly winds tend to move farther south and increase in intensity (Thompson and Wallace, 2000). This results in stronger cold water upwelling at high latitudes, anomalous downwelling

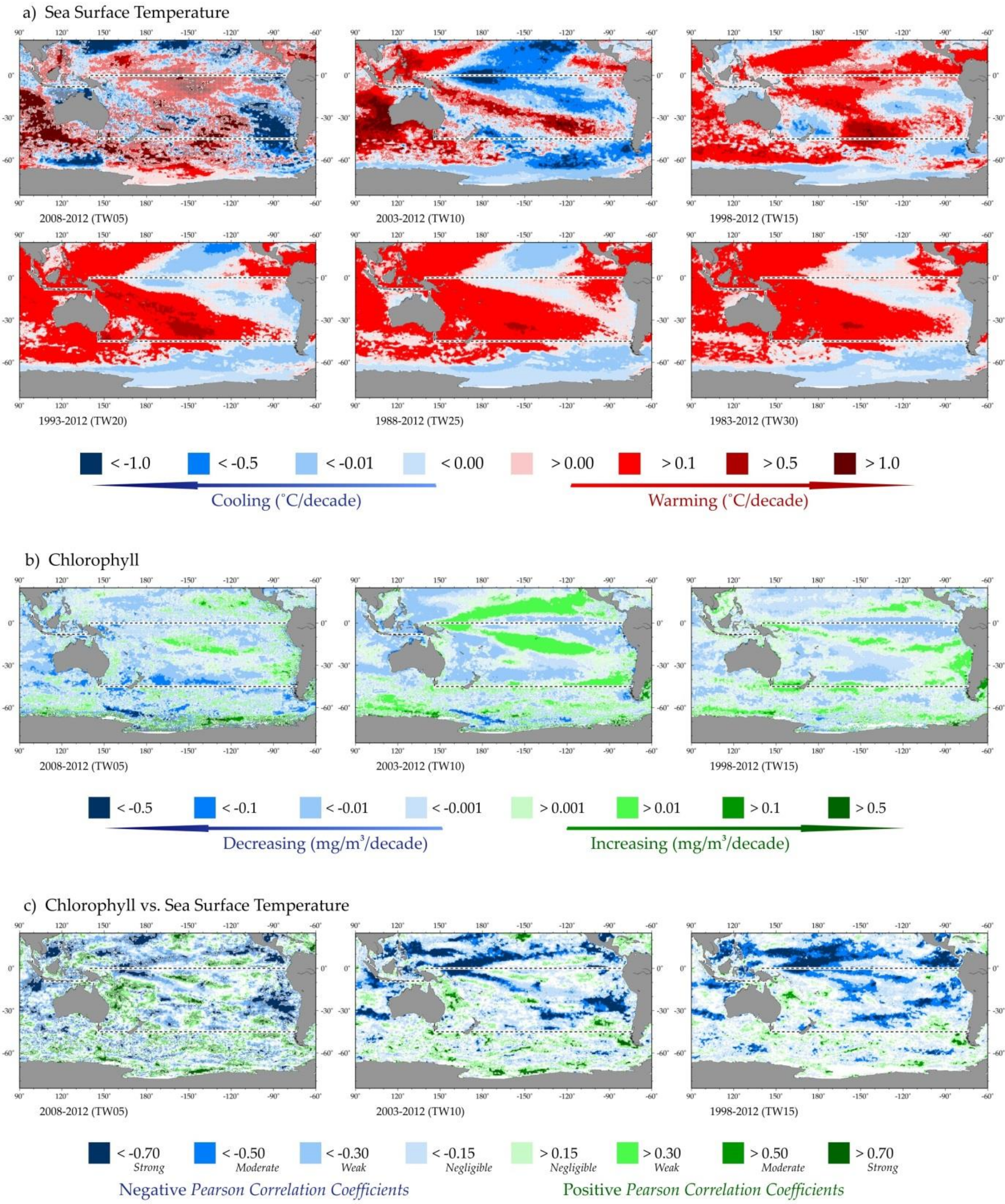

Figure 8.3. Annual trends in South Pacific sea surface temperature (SST) (a) and sea surface chlorophyll (CHL) (b), and correlations between chlorophyll and sea surface temperature for each of the standard IGMETS time-windows (c). See “Methods” chapter for a complete description and methodology used.

around 45°S, and a strengthening of the Antarctic Circumpolar Current (Hall and Visbeck, 2002; Oke and England, 2004). Variations in the SAM have been shown to be correlated with SST anomalies in the central tropical Pacific (Ding *et al.*, 2012). There is significant temporal variability in the SAM, but over the last 50+ years, the SAM index has been positive and on the rise (Thompson and Wallace, 2000; Abram *et al.*, 2014). This rise has been linked to anthropogenic factors which include ozone depletion (Fyfe *et al.*, 1999).

The following sections describe spatial and temporal patterns in temperature and chlorophyll *a* observed during 1983–2012 in the South Pacific as well as patterns in the biogeochemistry and ecology of the region as seen from satellite and ship-based time-series data compiled by IGMETS. How these may relate to ocean circulation and climate drivers is also explored. More detailed tables and maps can be obtained from the IGMETS Explorer tool (http://igmets.net/explorer/).

8.2 General patterns of temperature and phytoplankton biomass

8.2.1 30-year trends in SST

Over the past 30 years (1983–2012), 84.4% of the South Pacific has warmed (Figure 8.3; Table 8.1), of which 67.3% was significant ($p < 0.05$). Although the spatial extent of warming was substantial, it was more limited than in the Indian, Arctic or Atlantic oceans. Long-term, 30-year warming was most pronounced in the western Pacific, spanning from the equator to 50°S along 150°E. This large area of warming extended eastward from Australia toward South America, but also contracted poleward. There was another smaller region of warming at the equator around 95°W. Close to the South American continent, there were two regions of persistent cooling: a larger one off northern Chile and southern Peru (ca. 10–30°S) and a smaller one at ca. 40–50°S. Over the 30-, 25-, and 20-year temporal windows, the larger cooling region extended west and north all the way to the equator (Figure 8.2).

This spatial pattern of warm and cool areas was mostly driven by a combination of long-term global warming and changes in the phase of the Interdecadal Pacific Oscillation (IPO; Dong and Zhou, 2014; Dong and Dai, 2015). The multidecadal cooling trend was associated with a change in phase of IPO from positive to negative around 1998/1999 (Dong and Zhou, 2014) as well as more frequent occurrences of central Pacific-type El Niño events (Chavez *et al.*, 2003; Sohn *et al.*, 2013). The change in the IPO also enhanced the east–west thermal contrast that produced an intensification of global monsoon precipitation (Wang *et al.*, 2012b), trade winds across the Pacific (England *et al.*, 2014), and a greater contrast in sea level pressure (SLP) between the eastern and western tropical Pacific (Merrifield, 2011). These changes in surface wind, precipitation, and SLP in the tropical Pacific over the past 30 years may also have led to a general increase in the Walker circulation (Liu and Curry, 2006; Sohn and Park, 2010; Sohn *et al.*, 2013; Kosaka and Xie, 2013). The fact that over 80% of the South Pacific warmed since 1983, however, suggests that global warming dominated over the ENSO, IPO, and SAM cycles.

8.2.2 15-, 10-, and 5-year trends in SST

Over the periods 1998–2012 and 2003–2012 (15- and 10-year windows, respectively), a strong band of warming was visible extending roughly along the trajectory of the SPCZ south and east from Papua New Guinea to about 100°W (Figure 8.3). The area of South Pacific warming over the 15-year time-window was 65.1% (Table 8.1; Figure 8.3). Between 2003 and 2012, the spatial extent of warming was reduced to only 36.7%, and the majority of the South Pacific (63.3%) was cooling at a rate of –0.1°C year^{-1}. Over this 10-year period, some of the strongest cooling trends were in the region of the western Pacific warm pool (Figure 8.3; Table 8.1). This decadal cooling trend has been largely attributed to La Niña-like conditions (Kosaka and Xie, 2013), the negative phase of the IPO (Dong and Zhou, 2014; Meehl *et al.*, 2014), and a strengthening in Pacific trade winds (England *et al.*, 2014). During the shorter 5-year window (2008–2012), the cooling still prevailed, but only over 50.4% of the South Pacific (Figure 8.3; Table 8.1).

Table 8.1. Relative spatial areas (% of the total region) and rates of change within the South Pacific region that are showing increasing or decreasing trends in sea surface temperature (SST) for each of the standard IGMETS time-windows. Numbers in brackets indicate the % area with significant ($p < 0.05$) trends. See "Methods" chapter for a complete description and methodology used.

Latitude-adjusted SST data field surface area = 68.8 million km²	**5-year** (2008–2012)	**10-year** (2003–2012)	**15-year** (1998–2012)	**20-year** (1993–2012)	**25-year** (1988–2012)	**30-year** (1983–2012)
Area (%) w/ increasing SST trends ($p < 0.05$)	**50.4%** (5.6%)	36.7% (15.5%)	**65.1%** (31.0%)	**67.4%** (52.1%)	**88.3%** (68.1%)	**84.4%** (67.3%)
Area (%) w/ decreasing SST trends ($p < 0.05$)	49.6% (12.2%)	**63.3%** (38.4%)	34.9% (14.7%)	32.6% (11.8%)	11.7% (0.7%)	15.6% (5.3%)
> 1.0°C decade⁻¹ warming ($p < 0.05$)	11.2% (4.5%)	0.9% (0.9%)	0.3% (0.3%)	0.0% (0.0%)	0.0% (0.0%)	0.0% (0.0%)
0.5 to 1.0°C decade⁻¹ warming ($p < 0.05$)	15.5% (1.1%)	8.2% (7.7%)	5.6% (5.6%)	8.1% (8.1%)	1.2% (1.2%)	0.9% (0.9%)
0.1 to 0.5°C decade⁻¹ warming ($p < 0.05$)	18.3% (0.1%)	20.9% (6.9%)	41.5% (24.6%)	45.6% (42.6%)	**61.9%** (60.7%)	**58.7%** (58.2%)
0.0 to 0.1°C decade⁻¹ warming ($p < 0.05$)	5.4% (0.0%)	6.7% (0.1%)	17.7% (0.5%)	13.6% (1.4%)	25.3% (6.1%)	24.8% (8.3%)
0.0 to –0.1°C decade⁻¹ cooling ($p < 0.05$)	5.3% (0.0%)	7.7% (0.2%)	13.0% (0.2%)	18.9% (1.7%)	10.9% (0.2%)	14.3% (4.0%)
–0.1 to –0.5°C decade⁻¹ cooling ($p < 0.05$)	16.7% (0.4%)	33.6% (17.5%)	20.7% (13.3%)	13.7% (9.9%)	0.7% (0.5%)	1.3% (1.3%)
–0.5 to –1.0°C decade⁻¹ cooling ($p < 0.05$)	13.8% (2.8%)	18.8% (17.6%)	1.2% (1.2%)	0.1% (0.1%)	0.0% (0.0%)	0.0% (0.0%)
> –1.0°C decade⁻¹ cooling ($p < 0.05$)	13.8% (9.1%)	3.1% (3.1%)	0.0% (0.0%)	0.0% (0.0%)	0.0% (0.0%)	0.0% (0.0%)

Table 8.2. Relative spatial areas (% of the total region) and rates of change within the South Pacific region that are showing increasing or decreasing trends in phytoplankton biomass (CHL) for each of the standard IGMETS time-windows. Numbers in brackets indicate the % area with significant ($p < 0.05$) trends. See "Methods" chapter for a complete description and methodology used.

Latitude-adjusted CHL data field surface area = 68.8 million km²	**5-year** (2008–2012)	**10-year** (2003–2012)	**15-year** (1998–2012)
Area (%) w/ increasing CHL trends ($p < 0.05$)	27.0% (6.0%)	39.4% (22.1%)	41.5% (20.0%)
Area (%) w/ decreasing CHL trends ($p < 0.05$)	**73.0%** (36.3%)	**60.6%** (39.9%)	**58.5%** (40.4%)
> 0.50 mg m⁻³ decade⁻¹ increasing ($p < 0.05$)	0.2% (0.1%)	0.0% (0.0%)	0.1% (0.1%)
0.10 to 0.50 mg m⁻³ decade⁻¹ increasing ($p < 0.05$)	1.4% (0.5%)	0.5% (0.4%)	1.0% (0.9%)
0.01 to 0.10 mg m⁻³ decade⁻¹ increasing ($p < 0.05$)	15.6% (5.3%)	23.4% (18.8%)	16.1% (13.0%)
0.00 to 0.01 mg m⁻³ decade⁻¹ increasing ($p < 0.05$)	9.8% (0.2%)	15.4% (2.9%)	24.3% (6.1%)
0.00 to –0.01 mg m⁻³ decade⁻¹ decreasing ($p < 0.05$)	13.7% (1.8%)	22.3% (8.7%)	33.6% (18.0%)
–0.01 to –0.10 mg m⁻³ decade⁻¹ decreasing ($p < 0.05$)	**52.4%** (29.2%)	36.8% (30.0%)	24.5% (22.0%)
–0.10 to –0.50 mg m⁻³ decade⁻¹ (decreasing) ($p < 0.05$)	6.5% (5.0%)	1.2% (0.9%)	0.5% (0.3%)
> –0.50 mg m⁻³ decade⁻¹ (decreasing) ($p < 0.05$)	0.4% (0.3%)	0.3% (0.3%)	0.0% (0.0%)

8.2.3 15-year trends in chlorophyll *a*

The dominant trend for surface chlorophyll *a* has been to decline in the South Pacific (Figure 8.3; Table 8.2). The South Pacific, however, had regions of positive and negative trends in chlorophyll *a*, depending on the region and the temporal window considered. In the tropics, there was often a relationship between warming and declining chlorophyll *a*, while across most of the temporal windows and much of the South Pacific, significant relationships between SST and chlorophyll *a* were relatively rare (Figure 8.3, bottom). Over the 15-year time-window, chlorophyll *a* declined over 58.5% (40.4%, $p < 0.05$) of the South Pacific. Most of this decline occurred in the South Pacific gyre or in the tropical eastern Pacific (Figure 8.3). The South Pacific gyre itself has been estimated to be growing at 245 766 km^2 $year^{-1}$ (or 1.4% $year^{-1}$) between 1998 and 2006 (Polovina *et al.*, 2008). The decline in chlorophyll *a* within the tropical eastern Pacific was observed in a similar analysis by Gregg and Rousseaux (2014) and suggested to be linked to ENSO. Significant increases in chlorophyll *a* were observed at about 10°S and between 20 and 40°S off the coast of South America, along the Subtropical Front (STF) stretching from Tasmania to South America, and along the trajectory of the SPCZ. These observations agree with other findings based on satellite observations (Vantrepotte and Melin, 2011; Siegel *et al.*, 2013; Gregg and Rousseaux, 2014). Greater chlorophyll *a* concentrations in the Humboldt Current are consistent with suggestions of increasing upwelling intensity as a result of climate change (Bakun, 1990; Gutiérrez *et al.*, 2011; Sydeman *et al.*, 2014). The eddies along the STF appear to support substantial blooms of coccolithophores (Balch *et al.*, 2011, 2016) during austral summer (December–January). ENSO may also exert an influence on phytoplankton along the STF; for example, when a positive SAM aligns with a positive ENSO event, the eddy kinetic energy and number of eddies increases significantly (Langlais *et al.*, 2015). Over the 15-year time-window, the highest rate of chlorophyll *a* increase was > 0.01 mg chlorophyll *a* m^{-3} $year^{-1}$ measured in the southern Tasman Sea. This appears to be associated with greater EAC eddy pumping and an increase in winter intrusions of the STF into the Tasman Sea (Matear *et al.*, 2013; Kelly *et al.*, 2015).

8.2.3 10-year trends in chlorophyll *a*

Between 2003 and 2012, 60.6% (39.9% significant with $p < 0.05$) of the South Pacific showed a decline in chlorophyll *a* (Table 8.2; Figure 8.3). At the same time, a marked increase in chlorophyll *a* was observed in a band across the South Pacific from about 0°E and 160°E to 20°S and 100°W. The chlorophyll *a* increase overlapped part of the SPCZ, running north of, but parallel to, the band of strongly warming SST (Figure 8.3). A similar spatial pattern of increasing chlorophyll *a* was also evident over the 15 years between 1998 and 2012. There was a strikingly similar spatial pattern of temporal trends in temperature and chlorophyll *a* in the North Pacific (see Chapter 9, Figure 9.4) over this 100-year window. The cooler, more productive waters in the central South Pacific have been attributed, in part, to a strengthening of the Pacific trade winds (England *et al.*, 2014). At ca. 40–45°S off the coast of southern Chile, there was another region with a strong positive chlorophyll *a* trend over 10 years. This increase in chlorophyll *a* was positively correlated with SST (Figure 8.3).

Despite the cooler equatorial waters during the 10-year time-window, the upwelling zone of the tropical Pacific and off the Peruvian coast showed a decline in chlorophyll *a*. It has been suggested that this may be a result of ENSO (Gregg and Rousseaux, 2014). Finally, chlorophyll *a* patterns near the Chilean coast during this period were heterogeneous, but generally correlated negatively with temperature (Figure 8.3, bottom).

8.2.4 5-year trends in chlorophyll *a*

Over the most recent and shortest temporal window (2008–2012), declining chlorophyll *a* was observed over 73% (36.3% at $p < 0.05$) of the South Pacific (Table 8.2). Over this 5-year period, there were strong declines in chlorophyll *a* north of the STF and in the region of the western Pacific warm pool close to Papua New Guinea. Although considerably weaker, the spatial pattern of an increase in chlorophyll *a* spreading eastward and at an angle away from the equator across the Pacific was also evident over this time-window (Figure 8.3). A patchy, but broad, increase in remotely-sensed chlorophyll *a* was evident east of Australia through the southern Coral Sea and northern Tasman Sea as far east as 160°E (Figure 8.3). Some of these patches showed a strong positive correlation with SST. Explanations for these positive correlations in the open ocean are largely hypothetical, although predicted by some models and potentially attributable to (i) more diazotrophs (Dutkiewicz *et al.*, 2014), (ii) potential increase in eddy pumping (McGillicuddy *et al.*, 1998) associated with increasing eddy kinetic energy, and (iii) the strengthening of the EAC (Matear *et al.*, 2013). Sporadic increases in chlorophyll *a* were also observed off Chile in the region where the current flow along the STF interacts with the subtropical water mass.

8.3 Trends from *in situ* time series

In the western South Pacific, there are four *in situ* time series (Figure 8.4; Table 8.3), all in Australian waters (Lynch *et al.*, 2014). In addition, there are three *in situ* time series of phytoplankton and zooplankton data constructed from Continuous Plankton Recorder routes along the Australian shelf break. The Australian time series commenced after 2007 and only have data for the 5-year temporal window (2008–2012). The tropical site of Yongala (19°S) off northeast Australia is within the Great Barrier Reef Lagoon and broadly influenced by coastal processes. Yongala showed increasing *in situ* temperatures during 2008–2012. Sites farther south at Port Hacking (34°S) and Maria Island (43°S) all cooled between 2008 and 2012 (Figure 8.4), reversing the longer-term trends for warming that had been measured in that region at a rate of ca. 0.75°C century^{-1} and 2.2°C century^{-1}, respectively (Thompson *et al.*, 2009). Generally, the waters along the east Australian continental shelf have been warming in association with the strengthening of the South Pacific gyre (Ridgway, 2007; Hill *et al.*, 2011). Where the shelf is narrow (Port Hacking) or the STF periodically intrudes (Maria Island), however, the short-term or local trends can vary.

Table 8.3. Five-year trends (TW05, 2008–2012) in the time series of observations from the *in situ* sites in the South Pacific (not including Continuous Plankton Recorder sites).

Site-ID	Lat (°E) Long (°S)	SST	S	Oxy	NO3	CHL	Cope-pods	Dia.	Dino.	Dia.: Dino.
au-50109 Yongala	19.18 147.37	+	+	n/a	n/a	+	-	+	-	+
au-50107 North Stradbroke Island	27.20 153.33	n/a	-	n/a	+	-	+	-	-	-
au-50101 Port Hacking	34.05 151.15	-	+	n/a	+	+	n/a	-	-	-
au-50105 Maria Island	42.35 148.14	-	+	-	+	+	+	-	-	-
cl-30101 Concep-tion 18	36.50 73.00	n/a	n/a	n/a	n/a	n/a	n/a	n/a	n/a	n/a
cl-30102 Bay of Mejillones	23.10 70.47	n/a	n/a	n/a	n/a	n/a	n/a	n/a	n/a	n/a
pe-30101 IMARPE A	4.80 82.00	n/a	n/a	n/a	n/a	n/a	n/a	n/a	n/a	n/a
pe-30102 IMARPE B	9.00 79.00	n/a	n/a	n/a	n/a	n/a	n/a	n/a	n/a	n/a
pe-30103 IMARPE C	16.00 75.00	n/a	n/a	n/a	n/a	n/a	n/a	n/a	n/a	n/a
pe-30104 IMARPE Callao	11.99 78.97	n/a	n/a	+	-	-	n/a	n/a	n/a	n/a

$p > 0.05$ negative positive $p < 0.05$ negative positive

From 2008 to 2012, *in situ* salinity trends were weak, tending to increase at three sites and decline at one site along the east coast of Australia (Figure 8.4). Over the same time-period, nitrate concentrations increased weakly at three mid-latitude stations (North Stradbroke Island, Port Hacking, and Maria Island). Nitrate concentrations at Pork Hacking have been rising since the 1950s (Thompson *et al*., 2009; Kelly *et al*., 2015). The strengthening EAC, a positive IPO, and the La Niña of 2010–2011 are likely to have reduced downwelling and shallowed the pynocline along the east coast of Australia (Gibbs *et al*., 1998), potentially providing more nutrients to the euphotic zone. Between 2008 and 2012, silicate concentrations increased at North Stradbroke Island, Port Hacking, and Maria Island, reversing strong 30-year declines at the latter two sites (Thompson *et al*., 2009). The La Niña event of 2011 broke the "Millennium Drought" for eastern Australia (Dijk *et al*., 2013), with the second highest rainfalls ever recorded and many rivers flooding over their banks. The increased silicate potentially reflects the input of substantial silicate-rich runoff.

Between 2008 and 2012, the *in situ* chlorophyll *a* concentrations rose significantly at three sites along the mid to northeast coast of Australia, while trends were weaker and mixed at sites farther south (Figure 8.4). The spatial footprint of Australian sites at North Stradbroke Island and Maria Island are known to reflect changes in chlorophyll *a* and temperature over broad regions of the South Coral Sea and Tasman Sea, respectively (Oke and Sakov, 2012; Jones *et al*., 2015). In some cases, the positive *in situ* chlorophyll *a* trends observed along the Australian coast contrasted with the weak trends measured using satellite remote sensing, highlighting the difference that may exist between these measurements in coastal areas and the need to use caution when interpreting data from just one source (Pennington *et al*., 2006).

Zooplankton and phytoplankton data from the east coast of Australia in 2008–2012 were available from seven sites where trends in total copepod biomass were mixed: four positive and three negative (Figure 8.3). The two significant positive trends in zooplankton from the CPR route on the mid-east coast coincided with *in situ* measurements of increasing chlorophyll *a* by CPR colour index. On the eastern coast of Australia (North Stradbroke Island site), a strong trend in increasing copepod biomass was also found, but with weakly decreasing *in situ* chlorophyll *a*. In addition, all three sites with increasing copepod biomass were in regions of increasing SST (Figure 8.3).

Off the Australian east coast, diatoms increased at three of seven sites (Figure 8.4g); the most significant increase was observed in offshore sites near the separation zone at about 30°S where most of the EAC turns eastward to flow across the Tasman Sea. Dinoflagellates also increased at these mid-coast sites. Trends at the more coastal and the most southerly stations tended to be weak and negative. The surface nutrient concentrations along the east coast of Australia are extremely low (Condie and Dunn, 2006), with low silicate previously reported to limit diatom blooms (Grant, 1971). Between the La Niña of 1999, during the millennium drought and prevailing El Niño conditions, diatoms declined significantly along Australia's east coast (Ajani *et al*., 2016). However, the 2008–2012 data suggest that diatoms recovered at Yongala, while dinoflagellates declined and the diatom/dinoflagellate ratio increased (Figures 8.4g, f; Table 8.3).

In the eastern South Pacific, *in situ* time series were scarce. Based on satellite data, the region has been broadly cooling throughout all temporal windows. At the Peruvian site of Callao (11°S), nutrients (nitrate, phosphate, and silicate) have generally declined, with nitrate and silicate decreasing from 1998 to 2012 (Figure 8.4). Callao also showed declines in chlorophyll *a* for the same time-period. The negative trend is consistent with satellite data. The recent decline in phytoplankton has been attributed to warmer conditions induced by the ENSO. Over the longer period of 15 years, the Callao time series of chlorophyll *a* was still negative, while the Bay of Mejillones showed a positive trend. Satellite data indicated that, during 1998–2012, the region was experiencing spatially heterogeneous increases (Vargas *et al*., 2007; Chavez and Messié, 2009; Chavez *et al*., 2011; Gutierrez *et al*., 2011) and decreases (Thomas *et al*., 2009) in chlorophyll *a* (Figure 8.3).

Two zooplankton time series were available along the west coast of South America from 23°S (Bay of Mejillones) and ca. 36°S (Concepción Station). The temporal trends in zooplankton biomass were generally weak, sometimes positive and sometimes negative. For example, a weak positive trend in zooplankton biomass was found over 15 years (1998–2012) in the Bay of Mejillones. The notable exception was a statistically significant, negative trend in zooplankton biomass off southern Chile at the Concepción site between 2003 and 2012.

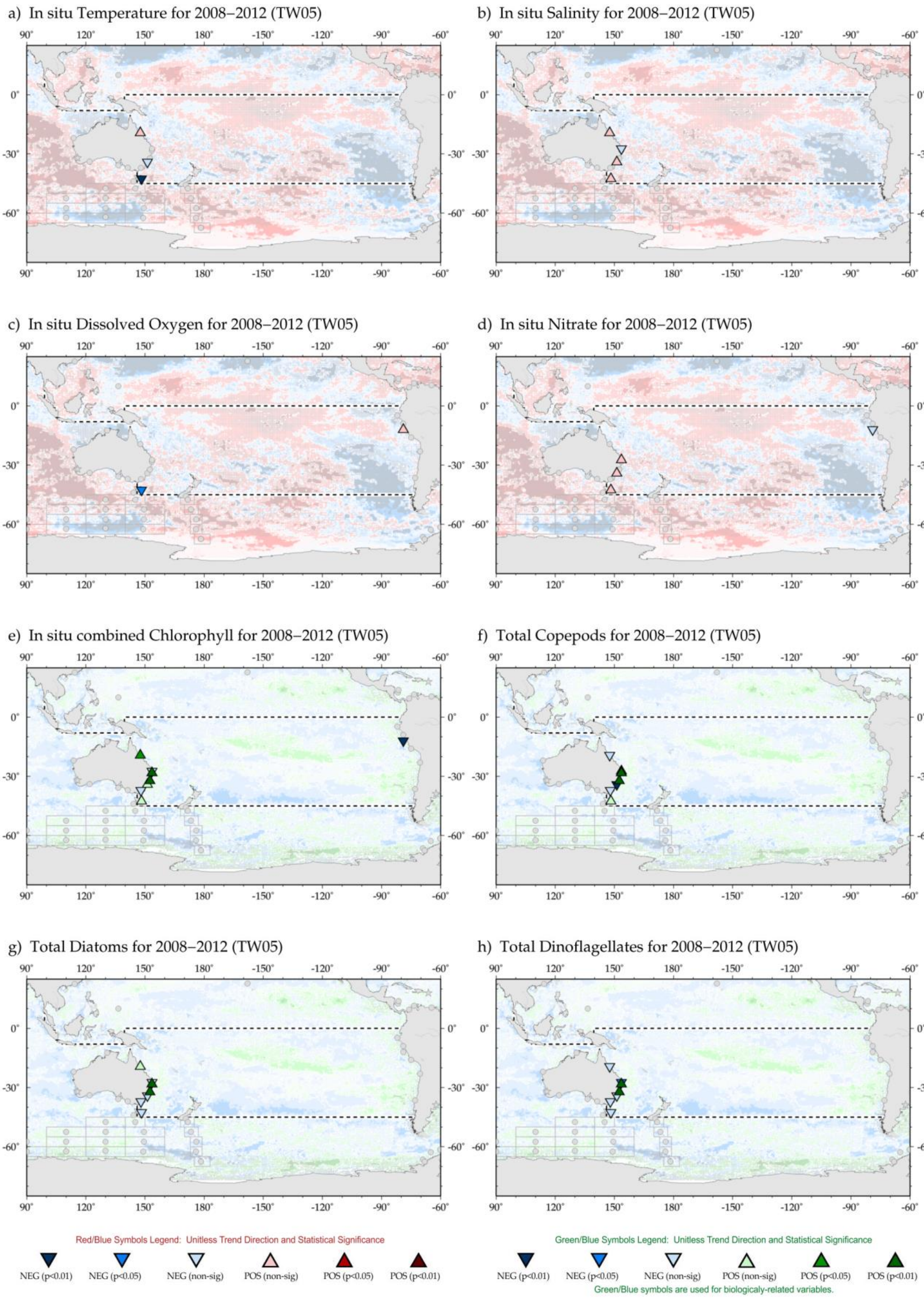

Figure 8.4. Map of South Pacific region time-series locations and trends for select variables and IGMETS time-windows. Upward-pointing triangles indicate positive trends; downward triangles indicate negative trends. Gray circles indicate time-series sites that fell outside of the current study region or time-window. Additional variables and time-windows are available through the IGMETS Explorer (http://IGMETS.net/explorer). See "Methods" chapter for a complete description and methodology used.

This trend occurred in spite of declining SST and increasing upwelling (Escribano *et al*., 2012). As noted by Escribano *et al*. (2012), zooplankton biomass is sensitive to the timing and scale of upwelling. Ayon *et al*. (2008) suggested that zooplankton biomass is positively correlated with seasonal temperature, and thus persistent upwelling may be a negative factor for zooplankton abundance. Zooplankton abundance rose 50% from 1981 to 2002 off Peru, but in 2002, it was still only one-fourth of the peak biomass observed in 1967 (Ayón *et al*., 2008). Ayón *et al*. (2008) also reported a positive correlation between zooplankton and anchovy biomass.

Dissolved oxygen (DO) trends were only available from two sites in the entire South Pacific: off Tasmania and in the Peruvian upwelling (Callao). Off Tasmania, the 2008–2012 trends were weakly negative. At ca. 11°S off Peru, DO trends were positive and statistically significant over the 15 years between 1998 and 2012. Combined with the declining SST (satellite data only), the 15 years of increasing DO observed at Callao support the hypothesis of a more vigorous upwelling in this boundary current in response to climate change (Bakun, 1990) and/or a response to the intensification of the trade winds in the Pacific (England *et al*., 2014).

8.4 Comparisons with other studies

The long-term rate of warming for southern hemisphere oceans has been 0.03°C decade^{-1} (Rayner *et al*., 2006), although across the entire South Pacific basin, this trend was found to be statistically insignificant over the last 60 years (Hoegh-Guldberg *et al*., 2014). Yet, the IGMETS analysis for 2008–2012 in the South Pacific showed 11.2% (4.5% at $p < 0.05$) of the surface ocean was warming at > 1.0°C decade^{-1} and a similar rate of cooling was found over 13.8% (9.1% at $p < 0.05$). Clearly, there is a need to consider subbasin-scale variability and the role of natural climatic cycles. These regional patterns in SST have been attributed to both human-induced global warming (Stott *et al*., 2010) and natural climatic cycles (e.g. IPO, ENSO; Dong and Zhou, 2014; England *et al*., 2014; Dong and Dai, 2015; Karl *et al*., 2015). The combination of progressive global warming, the IPO, and ENSO seem to account for most of the temporal and spatial patterns in SST trends observed over the last 30 years in the tropical Pacific (Dong and Dai, 2015).

The proportion of the South Pacific that is warming is rising much faster than the proportional increase in SST (Polovina and Woodworth, 2012). The long-term cooling SST trend in much of the eastern South Pacific is consistent with suggestions of increasing upwelling intensity as a result of climate change (Bakun, 1990; Sydeman *et al*., 2014), changes in the subtropical gyre circulation (Cai *et al*., 2005; Schneider *et al*., 2007), and changes in the Pacific wind regime (England *et al*., 2014). The dramatic cooling observed in this analysis over large parts of the South Pacific during the 2003–2012 time-window has also been noted by several studies and attributed to natural climate variability, tied specifically to La Niña-like decadal cooling (Kosaka and Xie, 2013) and wind-induced cooling (England *et al*., 2014). Natural climatic cycles have also affected surface salinity in the region. The negative IPO and strong La Niña of 2010–2011 saw a southwest shift in the SPCZ, bringing more precipitation to the South Pacific (Salinger *et al*., 2001; Folland *et al*., 2002; Cai and Rensch, 2012). At the same time, equatorial rainfall moved eastward along the ITCZ. Similarly, there has been a significant freshening in the western tropical Pacific, extending eastward under the low-salinity ITCZ and SPCZ regions (Durack and Wijffels, 2010).

The trends reported herein for satellite-derived chlorophyll *a* are similar to those previously published (Gregg and Conkright, 2002; Thomas *et al*., 2012; Siegel *et al*., 2013; Gregg and Rousseaux, 2014). For large portions of the South Pacific, there is a tendency for chlorophyll *a* to covary negatively with SST (Martinez *et al*., 2006; Vantrepotte and Mélin, 2011), a pattern consistent with warming SST being associated with a deeper surface mixed layer and reduced nutrient availability (Thomas *et al*., 2009; Hofmann *et al*., 2011, Doney *et al*., 2012). There were also regions of positive covariation between SST and chlorophyll *a* previously reported in the tropics north and west of Australia (Martinez *et al*., 2006) along the STF (Vantrepotte and Mélin, 2011) and in parts of the central gyre (Signorini *et al*., 2015). For regions where the mixed-layer depth is too deep for net positive phytoplankton growth during most of the year, e.g. along the STF, a positive relationship of chlorophyll *a* with SST is predictable. A similar covariation has been found in Humboldt Current off Peru and northern Chile (Thomas *et al*., 2009), where wind and chlorophyll phenology are out of phase and mixed-layer depth and light play a significant role in surface chlorophyll concentrations (Echevin *et al*., 2008). The major impacts of these changes are increasingly evident and amenable to modelling that accounts for both the physical supply and biological losses of carbon, oxygen, and nutrients (e.g. Deutsch *et* *al*., 2006, 2011). For example, changes in chlorophyll *a* within the Tasman Sea are well described in models and estimated into the future by climatic forcings (Matear *et al*., 2013). Climate-related changes to phytoplankton taxa have also been modelled (Bopp *et al*., 2005), statistically estimated (Barnes *et al*., 2011), extrapolated using remote sensing (Polovina and Woodworth, 2012; Uitz *et al*., 2015), and modelled using a combination of both (Gregg and Rouseaux, 2014). One general outcome that seems highly likely is a shift to smaller taxa as the oceans continue to warm (Barnes *et al*., 2011).

The tropical Pacific has seen a dramatic decline in oxygen concentration; some of the steepest declines were measured under the western Pacific warm pool, while the lowest concentrations were in the eastern tropical Pacific (Stramma *et al*., 2010). In 2012, the trend was observed as -1 µmol kg^{-1} year^{-1} between 2°N and 8°S at about 86°W (Czeschel *et al*., 2015). This oxygen consumption was associated with significantly increased phosphate and nitrate concentrations in the oxygen-minimum zone. The biological effects of the declining oxygen concentrations include vertical compression of habitat for species with high oxygen requirements such as tuna (Prince and Goodyear, 2006). The increasing nutrient concentrations at depth also imply the sequestering of more nutrients below a strengthening pycnocline, potentially reducing primary production. However, the extent of low oxygen regions in the Pacific has been linked to equatorial Pacific wind regime (Deutsch *et al*., 2014).

Previous analysis (Thompson *et al*., 2009) showed mostly increasing nutrient concentrations in the shelf waters of eastern Australia, results which are largely consistent with IGMETS. A notable exception was the detection of a change from declining to increasing silicate during 2008–2012 in the more recent IGMETS analysis. The mixed positive and negative trends observed for *in situ* nutrients may be associated with changes in circulation, thermocline depth, and/or changes in ecosystems induced by the different climate modes operating in the Pacific (Pennington *et al*., 2006; Chavez *et al*., 2011).

8.5 Conclusions

Long-term trends in fundamental characteristics of the environment, such as temperature and salinity, are increasingly evident. For example, over the past 30 years, significant surface warming has been recorded over nearly tenfold more area of the South Pacific than surface cooling (67.3% vs. 5.3%, respectively). A strong physical coupling with planktonic ecology and biology is evident in the South Pacific, with a dominant warming pattern and significantly declining phytoplankton populations. The southeastern Pacific upwelling system continues to show intensification (Vargas *et al*., 2007), while the tropical Pacific and subtropical gyre mostly exhibited declining trends in surface chlorophyll *a*. Prediction of the future ecological state of this important system requires understanding the physical drivers and their ecological consequences throughout the foodwebs, particularly the impact changes may have on ecosystem services at a regional scale. Modelling has been used to predict trends in phytoplankton community composition within the South Pacific (Polovina and Woodworth, 2012; Rousseaux and Gregg, 2015), but these have very limited taxonomic resolution. The time series included in IGMETS provide the means to test, validate, and improve ecological models of trophic links and trophic efficiency across an ample spectrum of phytoplankton and zooplankton taxonomic groups and predict potential changes that may occur within Pacific Ocean foodwebs in response to climate variability.

While "short" climate cycles such as ENSO have been associated with changes in copepod abundance in the Pacific (White *et al*., 1995, Thompson *et al*., 2015), reports of long-term trends in macrozooplankton biomass or taxa in the South Pacific are extremely rare (Ajani *et al*., 2016). In other ocean basins, there have been stronger links established between zooplankton community composition and climate-related increases in temperature (Richardson and Schoeman, 2004; Chiba *et al*., 2006). Some researchers have also suggested links between the abundance of some jellyfish (Cnidaria) and climate (Richardson, 2008), but the hypothesis is supported by only a few case studies from other oceans (reviewed by Purcell, 2005). For this section, zooplankton data were available only in a handful of locations, and the same is true for most of the other biogeochemical and ecological variables. Indeed, our understanding of the climatic effects on marine ecology, such as phytoplankton community composition, zooplankton productivity, and fish populations in the South Pacific remains rudimentary mostly due to a lack of data. Our knowledge of the spatial scale of ecological changes is limited to a few regions with time-series data. For example, during the 2010 La Niña event, there was a poleward extension of some dominant tropical taxa, such as *Prochlorococcus* and *Synechococcus*, and a decline in macrozooplankton (Thompson *et al*., 2015). These apparent La Niña effects could have extended throughout the southwestern Pacific. Similarly, there have been large range expansions for some easily observed taxa such as *Noctiluca* (Thompson *et al*., 2009; Harrison *et al*., 2011; McLeod *et al*., 2012), raising concerns about rapid, but unobserved, changes in the basic ecology of our oceans (Doney *et al*., 2012). These very substantial expansions in regions of rapid warming suggest that physical transport of suitable habitat may be the controlling mechanism. The location of existing time series in the South Pacific also limits our knowledge of ecological changes to the continental shelf. While coastal sites can be used to warn of changes, such as low oxygen and high carbon dioxide water coming near shore (Chan *et al*., 2008), given the rapid rate of expanding low oxygen zones, it may be beneficial to have more offshore monitoring (Deutsch *et al*., 2015).

Table 8.4. Time-series sites located in the IGMETS South Pacific region. Participating countries: Argentina (ar), Brazil (br), Namibia (na), United Kingdom (uk), South Africa (za), Australia (au), Chile (il), and Peru (pe). Year-spans indicated in red belong to time series which were terminated. Year-spans in red text indicate time series of unknown or discontinued status. IGMETS-IDs in red text indicate time series without a description entry in Annex 6.

No.	IGMETS-ID	Site or programme name	Year-span	T	S	Oxy	Ntr	Chl	Mic	Phy	Zoo
1	au-40201	AusCPR BRSY Line – North (*Australian Coastline*)	2009–present	-	-	-	-	X	-	X	X
2	au-40202	AusCPR BRSY Line – South (*Australian Coastline*)	2009–present	-	-	-	-	X	-	X	X
3	au-40204	AusCPR SYME Line – South (*Australian Coastline*)	2009–present	-	-	-	-	X	-	X	X
4	au-50101	IMOS National Reference Station – Port Hacking (*Southeastern Australia*)	2002–present	X	X	-	X	X	X	X	X
5	au-50105	IMOS National Reference Station – Maria Island (*Tasmania*)	2009–present	X	X	X	X	X	X	X	X
6	au-50107	IMOS National Reference Station – North Stradbroke Island (*Eastern Australia*)	2008–present	-	X	-	X	X	X	X	X
7	au-50109	IMOS National Reference Station – Yongala (*Northeastern Australia*)	2009–present	X	X	-	X	X	X	X	X
8	cl-30101	Concepcion Station 18 (*Chilean Coast*)	2002–present	-	-	-	-	-	-	-	X
9	cl-30102	Bay of Mejillones (*Chilean Coast*)	1988–present	-	-	-	-	-	-	-	X
10	pe-30101	IMARPE Region A (*Eastern South Pacific*)	1962–2005 (?)	-	-	-	-	-	-	-	X
11	pe-30102	IMARPE Region B (*Eastern South Pacific*)	1962–2005 (?)	-	-	-	-	-	-	-	X
12	pe-30103	IMARPE Region C (*Eastern South Pacific*)	1964–2005 (?)	-	-	-	-	-	-	-	X
13	pe-30104	IMARPE Callao (*Eastern South Pacific*)	2001–present	-	-	X	X	X	-	-	-

8.6 References

Abram, N. J., Mulvaney, R., Vimeux, F., Phipps, S. J., Turner, J., and England, M. H. 2014. Evolution of the Southern Annular Mode during the past millennium. Nature Climate Change, 4: 564–569.

Ajani, P., Hallegraeff, G. M., Allen, D., Coughlan, A., Richardson, A. J., Armand, L. K., Ingelton, T., *et al*. 2016. Establishing baselines: a review of eighty years of phytoplankton diversity and biomass in south-eastern Australia. Oceanography and Marine Biology: An Annual Review, 54: 387–412.

Ayón, P., Criales-Hernandez, M. I., Schwamborn, R., and Hirche, H-J. 2008. Zooplankton research off Peru: A review. Progress in Oceanography, 79(2): 238–255.

Bakun, A. 1990. Global climate change and intensification of coastal ocean upwelling. Science, 247: 198–201.

Balch, W. M., Bates, N. R., Lam, P. J., Twining, B. S., Rosengard, S. Z., Bowler, B. C., Drapeau, D. T., *et al*. 2016. Factors regulating the Great Calcite Belt in the Southern Ocean and its biogeochemical significance. Global Biogeochemical Cycles, 30: doi:10.1002/2016GB005414.

Balch, W. M., Drapeau, D. T., Bowler, B. C., Lyczkowski, E., Booth, E. S., and Alley, D. 2011. The contribution of coccolithophores to the optical and inorganic carbon budgets during the Southern Ocean Gas Exchange Experiment: new evidence in support of the "Great Calcite Belt" hypothesis. Journal of Geophysical Research, 116: C00F06, doi:10.1029/2011JC006941.

Barnes, C., Irigoien, X., De Oliveira, J. A. A., Maxwell, D., and Jennings, S. 2011. Predicting marine phytoplankton community size structure from empirical relationships with remotely sensed variables. Journal of Plankton Research, 33: 13–24.

Biondi, F., Gershunov, A., and Cayan, D. R. 2001. North Pacific decadal climate variability since 1661. Journal of Climate, 14(1): 5–10, doi:10.1175/1520-442(2001)014.

Bopp, L., Aumont, O., Cadule, P., Alvain, S., and Gehlen, M. 2005. Response of diatoms distribution to global warming and potential implications: A global model study. Geophysical Research Letters, 32(19): doi:10.1029/2005GL023653.

Brown, J. R., Power, S. B., Delage, F. P., Colman, R. A., Moise, A. F., and Murphy, B. F. 2011. Evaluation of the South Pacific Convergence Zone in IPCC AR4 climate model simulations of the twentieth century. Journal of Climate, 24(6): 1565–1582, doi:10.1175/2010JCLI3942.1.

Cai, W., and Rensch, P. 2012. The 2011 southeast Queensland extreme summer rainfall: a confirmation of a negative Pacific Decadal Oscillation phase? Geophysical Research Letters, 39(8): doi:10.1029/2011GL050820.

Cai, W. J., Shi, G., Cowan, T., Bi, D. and Ribbe, J. 2005. The response of southern annular mode, the East Australian Current, and the southern midlatitude ocean circulation to global warming. Journal of Geophysical Research Letters, 32: doi:10.1029/2005GL024701.

Cetina-Heredia, P., Roughan, M., van Sebille, E., and Coleman, M. A. 2014. Long-term trends in the East Australian Current separation latitude and eddy driven transport. Journal of Geophysical Research: Oceans, 119: doi:10.1002/2014JC010071.

Chan, F., Barth, J. A., Lubchenco, J., Kirincich, A., Weeks, H., Peterson, W. T., and Menge, B. A. 2008. Emergence of anoxia in the California Current large marine ecosystem. Science, 319(5865): 920–920.

Chavez F. P., and Messié, M. 2009. A comparison of eastern boundary upwelling ecosystems. Progress in Oceanography, 83: 80–96.

Chavez, F. P., Messié, M., and Pennington, J. T. 2011. Marine primary production in relation to climate variability and change. Annual Review of Marine Science, 3: 227–260.

Chavez, F. P., Ryan, J., Lluch-Cota, S. E., and Ñiquen, M. 2003. From anchovies to sardines and back: multidecadal change in the Pacific Ocean. Science, 299(5604): 217–221.

Chiba, S., Tadokoro, K., Sugisaki, H., and Saino, T. 2006. Effects of decadal climate change on zooplankton over the last 50 years in the western subarctic North Pacific. Global Change Biology, 12(5): 907–920.

Condie, S. A., and Dunn, J. R. 2006. Seasonal characteristics of the surface mixed layer in the Australasian region: implications for primary production regimes and biogeography. Marine and Freshwater Research, 57(6): 569–590.

Correa-Ramirez, M. A., Hormazabal, S. E., and Morales, C. E. 2012. Spatial patterns of annual and interannual surface chlorophyll-a variability in the Peru–Chile Current System. Progress in Oceanography, 92: 8–17.

Czeschel, R., Stramma, L., Weller, R. A., and Fischer, T. 2015. Circulation, eddies, oxygen, and nutrient changes in the eastern tropical South Pacific Ocean. Ocean Science, 11: 455–470, doi:10.5194/os-11-455-2015.

Dai, A., Fyfe, J. C., Xie, S. P., and Dai, X. 2015. Decadal modulation of global surface temperature by internal climate variability. Nature Climate Change, 5(6): 555–559, doi:10.1038/nclimate2605.

Daneri, G., Dellarossa, V., Quiñones, R., Jacob, B., Montero, P., and Ulloa, O. 2000. Primary production and community respiration in the Humboldt Current System off Chile and associated oceanic areas. Marine Ecology Progress Series, 197: 41–49.

Deutsch, C., Berelson, W., Thunell, R., Weber, T., Tems, C., McManus, J., Crusius, J., *et al*. 2014. Centennial changes in North Pacific anoxia linked to tropical trade winds. Science, 345(6197): 665–668.

Deutsch, C., Brix, H., Ito, T., Frenzel, H., and Thompson, L. 2011. Climate-forced variability of ocean hypoxia. Science, 333(6040): 336–339.

Deutsch, C., Emerson, S., and Thompson, L. 2006. Physical-biological interactions in North Pacific oxygen variability. Journal of Geophysical Research: Oceans, 111: C09S90, doi:10.1029/2005JC003179.

Deutsch, C., Ferrel, A., Seibel, B., Pörtner, H. O., and Huey, R. B. 2015. Climate change tightens a metabolic constraint on marine habitats. Science, 348(6239): 1132–1135.

Dijk, A. I., Beck, H. E., Crosbie, R. S., Jeu, R. A., Liu, Y. Y., Podger, G. M., Timbal, B., *et al*. 2013. The Millennium Drought in southeast Australia (2001–2009): Natural and human causes and implications for water resources, ecosystems, economy, and society. Water Resources Research, 49(2): 1040–1057.

Ding, Q., Steig, E. J., Battisti, D. S., and Wallace, J. M. 2012. Influence of the tropics on the Southern Annular Mode. Journal of Climate, 25(18): 6330–6348, doi:http://dx.doi.org/10.1175/JCLI-D-11-00523.1.

Doney, S. C., Ruckelshaus, M., Duffy, J., Barry, J. P., Chan, F., English, C. A., Galindo, H. M., *et al*. 2012. Climate change impacts on marine ecosystems. Annual Review of Marine Science, 4: 11–37, doi:10.1146/annurev-marine-041911-111611.

Dong, B., and Dai, A. 2015. The influence of the Interdecadal Pacific Oscillation on temperature and precipitation over the globe. Climate Dynamics, 45(9-10): 2667–2681, doi:10.1007/s00382-015-2500-x.

Dong, L., and Zhou, T. 2014. The formation of the recent cooling in the eastern tropical Pacific Ocean and the associated climate impacts: A competition of global warming, IPO, and AMO. Journal of Geophysical Research: Atmosphere, 119: 11272–11287, doi:10.1002/2013JD021395.

Durack, P. J., and Wijffels, S. E. 2010. Fifty-year trends in global ocean salinities and their relationship to broad-scale warming. Journal of Climate, 23(16): 4342–4362, http://dx.doi.org/10.1175/2010JCLI3377.1.

Dutkiewicz, S., Ward, B. A., Scott, J. R., and Follows, M. J. 2014. Understanding predicted shifts in diazotroph biogeography using resource competition theory. Biogeosciences, 11: 5445–5461, doi:10.5194/bg-11-5445-2014.

Echevin, V., Aumont, O., Ledesma, J., and Flores, G. 2008. The seasonal cycle of surface chlorophyll in the Peruvian upwelling system: a modelling study. Progress in Oceanography, 79: 167–176.

England, M. H., McGregor, S., Spence, P., Meehl, G. A., Timmermann, A., Cai, W., Gupta, A. S., *et al*. 2014. Recent intensification of wind-driven circulation in the Pacific and the ongoing warming hiatus. Nature Climate Change, 4(3): 222–227.

Escribano, R., Hidalgo, P., Fuentes, M., and Donoso, K. 2012. Zooplankton time series in the coastal zone off Chile: Variation in upwelling and responses of the copepod community. Progress in Oceanography, 97–100: 174–186.

Fiedler, P. C., Philbrick, V., and Chavez, F. P. 1991. Oceanic upwelling and productivity in the eastern tropical Pacific. Limnology and Oceanography, 36: 1834–1850.

Folland, C. K., Renwick, J. A., Salinger, M. J., and Mullan, A. B. 2002. Relative influences of the Interdecadal Pacific Oscillation and ENSO in the South Pacific Convergence Zone. Geophysical Research Letters, 29: 21-1–21-4.

Fuenzalida, R., Schneider, W., Garcés-Vargas, J., and Bravo, L. 2008. Satellite altimetry data reveal jet-like dynamics of the Humboldt Current. Journal of Geophysical Research, 113: C07043, doi:10.1029/2007JC004684.

Fyfe, J. C., Boer, G. J., and Flato, G. M. 1999. Arctic and Antarctic oscillations and their projected changes under global warming. Geophysical Research Letters, 26(11): 1601–1604.

Gibbs, M. T., Middleton, J. H., and Marchesiello, P. 1998. Baroclinic response of Sydney shelf waters to local wind and deep ocean forcing, Journal of Physical Oceanography, 28: 178–190.

Grant, B. R. 1971. Variation in silicate concentration at Port Hacking station, Sydney, in relation to phytoplankton growth. Marine and Freshwater Research, 22(1): 49–54.

Godfrey, J. S., Cresswell, G. R., Golding, T. J., Pearce, A. F., and Boyd, R. 1980. The separation of the east Australian current. Journal of Physical Oceanography, 10(3): 430–440.

Gregg, W. W., and Conkright, M. E. 2002. Decadal changes in global ocean chlorophyll. Geophysical Research Letters, 29(11): 20–21, doi:10.1029/2002GL014689.

Gregg, W. W., and Rousseaux, C. S. 2014. Decadal trends in global pelagic ocean chlorophyll: A new assessment integrating multiple satellites, in situ data, and models. Journal of Geophysical Research: Oceans, 119: 5921–5933, doi:10.1002/2014JC010158.

Gutiérrez, D., Bouloubassi, I., Sifeddine, A., Purca, S., Goubanova, K., Graco, M., Field, D., *et al*. 2011. Coastal cooling and increased productivity in the main upwelling zone off Peru since the mid-twentieth century. Geophysical Research Letters, 38: L07603, doi:10.1029/2010GL046324.

Hall, A., and Visbeck, M. 2002. Synchronous variability in the Southern Hemisphere atmosphere, sea ice, and ocean resulting from the Annular Mode. Journal of Climate, 15(21): 3043–3057.

Harrison, P. J., Furuya, K., Glibert, P., Xu, J., Liu, H. B., Yin, K., Lee, J. H. W., *et al*. 2011. Geographical distribution of red and green Noctiluca scintillans. Chinese Journal of Oceanology and Limnology, 29: 807–831, doi:10.1007/s00343-011-0510-z.

Hasson, A., Delcroix, T., and Boutin, J. 2013. Formation and variability of the South Pacific Sea Surface Salinity maximum in recent decades. Journal of Geophysical Research: Oceans, 118: 5109–5116, doi:10.1002/jgrc.20367.

Hill, K. L., Rintoul, S. R., Ridgway, K., and Oke, P. R. 2011. Decadal changes in the South Pacific western boundary current system revealed in observations and reanalysis state estimates. Geophysical Research Letters, 116: doi: 10.1029/2009JC005926.

Hoegh-Guldberg, O., Cai, R., Poloczanska, E. S., Brewer, P. G., Sundby, S., Hilmi, K., Fabry, V. J., *et al*. 2014. The Ocean. *In* Climate Change 2014: Impacts, Adaptation, and Vulnerability. Part B: Regional Aspects, pp. 1655–1731. Ed. by V. R. Barros, C. B. Field, D. J. Dokken, M. D. Mastrandrea, K. J. Mach, T. E. Bilir, M. Chatterjee, *et al.* Contribution of Working Group II to the Fifth Assessment Report of the Intergovernmental Panel on Climate Change, Cambridge University Press, Cambridge and New York. 688 pp.

Hofmann, M., Worm, B., Rahmstorf, S., and Schellnhuber, H. J. 2011. Declining ocean chlorophyll under unabated anthropogenic CO_2 emissions. Environmental Research Letters, 6(3): 034035, doi:10.1088/1748-9326/3/034035.

Jones, E. M., Doblin, M. A., Matear, R., and King, E. 2015. Assessing and evaluating the ocean-colour footprint of a regional observing system. Journal of Marine Systems, 143: 49–61.

Karl, T. R., Arguez, A., Huang, B., Lawrimore, J. H., McMahon, J. R., Menne, M. J., Peterson, T. C., *et al*. 2015. Possible artifacts of data biases in the recent global surface warming hiatus. Science, 348(6242): 1469–1472.

Kelly, P., Clementson, L., and Lyne, V. 2015. Decadal and seasonal changes in temperature, salinity, nitrate, and chlorophyll in inshore and offshore waters along southeast Australia. Journal of Geophysical Research: Oceans, 120: 4226–4244.

Kosaka, Y., and Xie, S. P. 2013. Recent global-warming hiatus tied to equatorial Pacific surface cooling. Nature, 501(7467): 403–407.

Langlais, C., Rintoul, S., and Zika, J. 2015. Sensitivity of Antarctic circumpolar transport and eddy activity to wind patterns in the Southern Ocean. Journal Physical Oceanography, 45: 1051–1067, doi:10.1175/JPO-D-14-0053.1.

Liu, J., and Curry, J. A. 2006. Variability of the tropical and subtropical ocean surface latent heat flux during 1989–2000. Geophysical Research Letters, 33(5): doi: 10.1029/2005GL024809.

Lynch, T. P., Morello, E. B., Evans, K., Richardson, A. J., Rochester, W., Steinberg, C. R., Roughan, M., *et al*. 2014. IMOS national reference stations: a continental-wide physical, chemical and biological coastal observing system. PLoS ONE, 9(12): e113652, doi:10.1371/journal.pone.0113652.

Macdonald, H. S., Roughan, M., Baird, M. E., and Wilkin, J. 2013. A numerical modeling study of the East Australian Current encircling and overwashing a warm-core eddy. Journal of Geophysical Research: Oceans, 118: 301–315, doi:10.1029/2012JC008386.

Martinez, P., Lamy, F., Robinson, R. S., Pichevin, L., and Billy, I. 2006. Atypical δ15N variations at the southern boundary of the East Pacific oxygen minimum zone over the last 50 ka. Quaternary Science Reviews, 25: 3017–3028.

Mata, M. M., Tomczak, M., Wijffels, S., and Church, J. A. 2000. East Australian Current volume transports at 30 S: Estimates from the World Ocean Circulation Experiment hydrographic sections PR11/P6 and the PCM3 current meter array. Journal of Geophysical Research: Oceans, 105(C12): 28509–28526.

Mata, M. M., Wijffels, S. E., Church, J. A., and Tomczak, M. 2006. Eddy shedding and energy conversions in the East Australian Current. Journal of Geophysical Research, 111: C09034, doi:10.1029/2006JC003592.

Matear, R. J., Chamberlain, M. A., Sun, C., and Feng, M. 2013. Climate change projection of the Tasman Sea from an eddy-resolving ocean model. Journal of Geophysical Research, 118: 2961–2976, doi:10.1002/jgrc.20202.

McGillicuddy, D. J., Robinson, A. R., Siegel, D. A., Jannasch, H. W., Johnson, R., Dickeys, T., McNeil, J., *et al*. 1998. Influence of mesoscale eddies on new production in the Sargasso Sea. Nature, 394(6690): 263–266.

McLeod, D. J., Hallegraeff, G. M., Hosie, G. M., and Richardson, A. J. 2012. Climate-driven range expansion of the red-tide dinoflagellate *Noctiluca scintillans* into the Southern Ocean. Journal of Plankton Research, 34: 332–337.

McPhaden, M. J., Zebiak, S. E., and Glantz, M. H. 2006. ENSO as an integrating concept in earth science. Science, 314(5806): 1740–1745.

Meehl, G. A., Arblaster, J. M., Branstator, G., and van Loon, H. 2008. A coupled air–sea response mechanism to solar forcing in the Pacific region. Journal of Climate, 21: 2883–2897, doi:http://dx.doi.org/10.1175/2007JCLI1776.1.

Meehl, G. A., Teng, H., and Arblaster, J. M. 2014. Climate model simulations of the observed early-2000s hiatus of global warming. Nature Climate Change, 4(10): 898–902, doi:10.1038/nclimate2357.

Merrifield, M. A. 2011. A shift in western tropical Pacific sea level trends during the 1990s. Journal of Climate, 24(15): 4126–4138.

O'Kane, T. J., Oke, P. R., and Sandery, P. A. 2011. Predicting the east Australian current. Ocean Modelling, 38(3): 251–266, doi:10.1016/j.ocemod.2011.04.003.

Oke, P. R., and England, M. H. 2004. Oceanic response to changes in the latitude of the Southern Hemisphere subpolar westerly winds. Journal of Climate, 17(5): 1040–1054.

Oke, P. R., and Sakov, P. 2012. Assessing the footprint of a regional ocean observing system. Journal of Marine Systems, 105–108: 30–51.

Pennington, J. T., Mahoney, K. L., Kuwahara, V. S., Kolber, D. D., Calienes, R., and Chavez, F. P. 2006. Primary production in the eastern tropical Pacific: a review. Progress in Oceanography, 69: 285–317.

Philander, S. G. 1990. El Nino, La Niña, and the Southern Oscillation. Academic Press, San Diego. 293 pp.

Polovina, J. J., Howell, E. A., and Abecassis, M. 2008. The ocean's least productive waters are expanding. Geophysical Research Letters, 35: L03618, http://dx.doi.org/10.1029/2007GL031745.

Polovina, J. J., and Woodworth, P. A. 2012. Declines in phytoplankton cell size in the subtropical oceans estimated from satellite remotely-sensed temperature and chlorophyll, 1998–2007, Deep-Sea Research II, 77–80: 82–88, http://dx.doi.org/10.1016/j.dsr2.2012.04.006.

Prince, E. D., and Goodyear, C. P. 2006. Hypoxia-based habitat compression of tropical pelagic fishes. Fisheries Oceanography, 15(6): 451–464.

Purcell, J. E. 2005. Climate effects on formation of jellyfish and ctenophore blooms: a review. Journal of the Marine Biological Association of the United Kingdom, 85: 461–476.

Rasmusson, E. M., and Carpenter, T. H. 1982. Variations in tropical sea surface temperature and surface wind fields associated with the Southern Oscillation/El Nino. Monthly Weather Review, 110: 354–384.

Rayner, N. A., Parker, D. E., Horton, E. B., Folland, C. K., Alexander, L. V., Rowell, D. P., Kent, E. C., *et al.* 2003. Global analyses of sea surface temperature, sea ice, and night marine air temperature since the late nineteenth century. Journal of Geophysical Research, 108(D14): 4407, doi:10.1029/2002JD002670.

Rayner, N. A., Brohan, P., Parker, D. E., Folland, C. K., Kennedy, J. J., Vanicek, M., Ansell, T. J., *et al*. 2006. Improved analyses of changes and uncertainties in sea surface temperature measured *in situ* since the mid-nineteenth century: the HadSST2 dataset. Journal of Climate, 19: 446–469.

Richardson, A. 2008. In hot water: zooplankton and climate change. ICES Journal of Marine Science, 65(3): 279–295, doi:10.1093/icesjms/fsn028.

Richardson, A. J., and Schoeman, D. S. 2004. Climate impact on plankton ecosystems in the Northeast Atlantic. Science, 305(5690): 1609–1612, doi:10.1126/science.1100958.

Ridgway, K. R. 2007. Long-term trend and decadal variability of the southward penetration of the East Australian Current. Geophysical Research Letters, 34: L13613, doi:10.1029/2007GL030393.

Ridgway, K. R., and Godfrey, J. S. 1997. Seasonal cycle of the East Australian Current. Journal of Geophysical Research, 102(C10): 22921–22936, doi:10.1029/97JC00227.

Roemmich, D., and Cornuelle, B. 1990. Observing the fluctuations of gyre-scale ocean circulation: a study of the subtropical South Pacific. Journal of Physical Oceanography, 20: 1919–1934, doi:http://dx.doi.org/10.1175/1520-0485(1990)020<1919:OTFOGS>2.0.CO;2.

Rousseaux, C. S., and Gregg, W. W. 2015. Recent decadal trends in global phytoplankton composition. Global Biogeochemical Cycles, 29: 1674–1688, doi: 10.1002/2015GB005139.

Salinger, M. J., Renwick, J. A., and Mullan, A. B. 2001. Interdecadal Pacific oscillation and south Pacific climate. International Journal of Climatology, 21(14): 1705–1721, doi:10.1002/joc.691.

Schneider, W., Fukasawa, M., Garcés-Vargas, J., Bravo, L., Uchida, H., Kawano, T., and Fuenzalida, R. 2007. Spin-up of South Pacific subtropical gyre freshens and cools the upper layer of the eastern South Pacific Ocean. Geophysical Research Letters, 34(24): L24606, doi:10.1029/2007GL031933,2007.

Siegel, D. A., Behrenfeld, M. J., Maritorena, S., McClain, C. R., Antoine, D., Bailey, S. W., Bontempi, P. S., *et al*. 2013. Regional to global assessments of phytoplankton dynamics from the SeaWiFS mission. Remote Sensing of Environment, 135: 77–91.

Signorini, S. R., Franz, B. A., and McClain, C. R. 2015. Chlorophyll variability in the oligotrophic gyres: mechanisms, seasonality and trends. Frontiers in Marine Science, 2(1): doi:10.3389/fmars.2015.000001.

Sohn, B. J., and Park, S. C. 2010. Strengthened tropical circulations in past three decades inferred from water vapor transport. Journal of Geophysical Research: Atmospheres, 115: D15112, doi:10.1029/2009JD013713.

Sohn, B. J., Yeh, S. W., Schmetz, J., and Song, H. J. 2013. Observational evidences of Walker circulation change over the last 30 years contrasting with GCM results. Climate Dynamics, 40(7–8): 1721–1732.

Stott, P. A., Gillett, N. P., Hegerl, G. C., Karoly, D. J., Stone, D. A., Zhang, X., and Zwiers, F. 2010. Detection and attribution of climate change: a regional perspective. Wiley Interdisciplinary Reviews: Climate Change, 1(2): 192–211.

Stramma, L., Schmidtko, S., Levin, L. A., and Johnson, G. C. 2010. Ocean oxygen minima expansions and their biological impacts. Deep-Sea Research I: Oceanographic Research Papers, 57(4): 587–595.

Sydeman, W. J., García-Reyes, M., Schoeman, D. S., Rykaczewski, R. R., Thompson, S. A., Black, B. A., and Bograd, S. J. 2014. Climate change and wind intensification in coastal upwelling ecosystems. Science, 345(6192): 77–80.

Thomas, A. C., Brickley, P., and Weatherbee, R. 2009. Interannual variability in chlorophyll concentrations in the Humboldt and California Current systems. Progress in Oceanography, 83(1–4): 386–392, doi: 10.1016/j.pocean.2009.07.020.

Thomas, A. C., Strub, P. T., Weatherbee, R. A., and James, C. 2012. Satellite views of Pacific chlorophyll variability: Comparisons to physical variability, local versus nonlocal influences and links to climate indices. Deep-Sea Research II, 77–80: 99–116, http://dx.doi.org/10.1016/j.dsr2.2012.04.008.

Thompson, D. W., and Wallace, J. M. 2000. Annular modes in the extratropical circulation. Part I: Month-to-month variability. Journal of Climate, 13(5): 1000–1016.

Thompson P. A., Baird, M. E., Ingleton, T., and Doblin, M. A. 2009. Long-term changes in temperate Australian coastal waters: implications for phytoplankton, Marine Ecological Progress Series, 394: 1–19, doi: 10.3354/meps08297.

Thompson, P. A., Bonham, P., Rochester, W., Doblin, M. A., Waite, A. M., Richardson, A., and Rousseaux, C. 2015. Climate variability drives plankton community composition changes: an El Niño to La Niña transition around Australia. Journal of Plankton Research, 37(5): 966–984, doi: 10.1093/plankt/fbv069.

Trenberth, K. E. 1997. The definition of El Niño. Bulletin of the American Meteorological Society, 78: 2771–2777.

Trenberth, K. E. 2015. Has there been a hiatus? Science, 349: 691–692.

Uitz, J., Stramski, D., Reynolds, R. A., and Dubranna, J. 2015. Assessing phytoplankton community composition from hyperspectral measurements of phytoplankton absorption coefficient and remote-sensing reflectance in open-ocean environments. Remote Sensing of Environment, 171: 58–74, doi:10.1016/j.rse.2015.09.027.

Vantrepotte, V., and Mélin, F. 2011. Inter-annual variations in the SeaWiFS global chlorophyll a concentration (1997–2007). Deep-Sea Research I, 58: 429–441.

Vargas, G., Pantoja, S., Rutllant, J. A., Lange, C. B., and Ortlieb, L. 2007. Enhancement of coastal upwelling and interdecadal ENSO-like variability in the Peru-Chile Current since late 19th century. Geophysical Research Letters, 34: L13607, doi:10.1029/2006GL028812.

Vincent, D. G. 1994. The South Pacific convergence zone (SPCZ): A review. Monthly Weather Review, 122(9): 1949–1970.

Vincent, E. M., Lengaigne, M., Menkes, C. E., Jourdain, N. C., Marchesiello, P., and Madec, G. 2011. Interannual variability of the South Pacific Convergence Zone and implications for tropical cyclone genesis. Climate Dynamics, 36(9–10): 1881–1896.

Wang, B., Liu, J., Kim, H. J., Webster, P. J., and Yim, S. Y. 2012b. Recent change of the global monsoon precipitation (1979–2008). Climate Dynamics, 39(5): 1123–1135.

Wang, C., Deser, C., Yu, J-Y., DiNezio, P., and Clement, A. 2012a. El Niño and Southern Oscillation (ENSO): A Review. *In* Coral Reefs of the Eastern Pacific: Persistence and Loss in a Dynamic Environment, pp. 85–106. Ed. by P. W. Glynn, D. P. Manzello, and I. C. Enochs. Springer Netherlands. 657 pp.

White, J. R., Zhang, X., Welling, L. A., Roman, M. R., and Dam, H. G. 1995. Latitudinal gradients in zooplankton biomass in the tropical Pacific at 140 W during the JGOFS EqPac study: Effects of El Niño. Deep-Sea Research II: Topical Studies in Oceanography, 42(2): 715–733.

Wijffels, S. E., Toole, J. M., and Davis, R. 2001. Revisiting the South Pacific subtropical circulation: A synthesis of World Ocean Circulation Experiment observations along 32°S. Journal of Geophysical Research, 106: 19481–19513.

Wyrtki, K. 1963. The horizontal and vertical field of motion in the Peru Current. Bulletin of the Scripps Institution of Oceanography, 8: 313–344.

Wyrtki, K. 1989. Some thoughts about the west Pacific warm pool. *In* Proceedings of the Western Pacific International Meeting and Workshop on Toga Coare, Nouméa, New Caledonia, 24-30 May 1989, pp. 99-109. Ed. by J. Picaut Joël, R. Lukas, and T. Delcroix. ORSTOM, Centre de Nouméa.